THE JOURNAL OF PHYSICAL CHEMISTRY Letters

Letter

pubs.acs.org/JPCL

Charge and Nuclear Dynamics Induced by Deep Inner-Shell Multiphoton Ionization of CH_3I Molecules by Intense X-ray Free-Electron Laser Pulses

Koji Motomura,[†] Edwin Kukk,[†,‡] Hironobu Fukuzawa,[†,§] Shin-ichi Wada,[§,∥] Kiyonobu Nagaya,[§,⊥] Satoshi Ohmura,[⊥] Subhendu Mondal,[†] Tetsuya Tachibana,[†] Yuta Ito,[†] Ryosuke Koga,[∥] Tsukasa Sakai,[⊥] Kenji Matsunami,[⊥] Artem Rudenko,[#] Christophe Nicolas,[▽] Xiao-Jing Liu,[▽] Catalin Miron,[▽,○] Yizhu Zhang,[◆] Yuhai Jiang,[◆] Jianhui Chen,[¶] Mailam Anand,[∫] Dong Eon Kim,[∫] Kensuke Tono,[⊗] Makina Yabashi,[§] Makoto Yao,[⊥] and Kiyoshi Ueda*[,†,§]

[†]Institute of Multidisciplinary Research for Advanced Materials, Tohoku University, Sendai 980-8577, Japan

[‡]Department of Physics and Astronomy, University of Turku, Turku FI-20014, Finland

[§]RIKEN SPring-8 Center, Sayo, Hyogo 679-5148, Japan

[∥]Department of Physical Science, Hiroshima University, Higashi-Hiroshima 739-8526, Japan

[⊥]Department of Physics, Kyoto University, Kyoto 606-8502, Japan

[#]J. R. Macdonald Laboratory, Department of Physics, Kansas State University, Manhattan, Kansas 66506, United States

[▽]Synchrotron SOLEIL, L'Orme des Merisiers, Saint-Aubin, BP 48, FR-91192 Gif-sur-Yvette Cedex, France

[○]Extreme Light Infrastructure - Nuclear Physics (ELI-NP), "Horia Hulubei" National Institute for Physics and Nuclear Engineering, 30 Reactorului Street, RO-077125 Măgurele, Jud. Ilfov, Romania

[◆]Shanghai Advanced Research Institute, Chinese Academy of Sciences, 201210 Shanghai, China

[¶]Shanghai Institute of Applied Physics, Chinese Academy of Sciences, 201800 Shanghai, China

[∫]Department of Physics, CASTECH, MPC-AS, POSTECH, Pohang, Korea

[⊗]Japan Synchrotron Radiation Research Institute (JASRI), Sayo, Hyogo 679-5198, Japan

Supporting Information

ABSTRACT: In recent years, free-electron lasers operating in the true X-ray regime have opened up access to the femtosecond-scale dynamics induced by deep inner-shell ionization. We have investigated charge creation and transfer dynamics in the context of molecular Coulomb explosion of a single molecule, exposed to sequential deep inner-shell ionization within an ultrashort (10 fs) X-ray pulse. The target molecule was CH_3I, methane sensitized to X-rays by halogenization with a heavy element, iodine. Time-of-flight ion spectroscopy and coincident ion analysis was employed to investigate, via the properties of the atomic fragments, single-molecule charge states of up to +22. Experimental findings have been compared with a parametric model of simultaneous Coulomb explosion and charge transfer in the molecule. The study demonstrates that including realistic charge dynamics is imperative when molecular Coulomb explosion experiments using short-pulse facilities are performed.

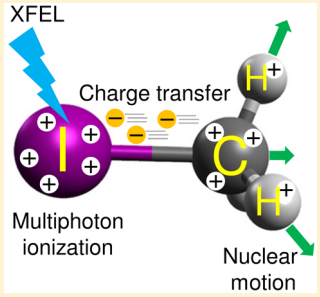

Two X-ray free-electron lasers (XFELs) are now in operation in the world. One is Linac Coherent Light Source (LCLS)[1] in USA and the other is SPring-8 Angstrom Compact free electron LAser (SACLA)[2] in Japan. They produce very intense yet extremely short X-ray pulses—a very suitable combination to perform damage-free X-ray imaging. The feasibility of single-shot coherent X-ray imaging of single nanosize macromolecules and particles,[3−7] and serial femtosecond X-ray diffraction (SFX) for protein nanocrystals[8−12] was indeed demonstrated at these facilities. These novel approaches are revolutionizing the field of structure determination and, as they venture into the hitherto unfamiliar regime of X-ray and matter interaction, are concurrently provoking considerable interest in the femtosecond-scale electron and nuclear dynamics, particularly in respect to radiation damage.[13−15]

With free-electron lasers at the extreme ultraviolet (EUV) wavelengths (such as FLASH in Germany and SCSS in Japan), the interaction of atoms and molecules with intense ultrashort EUV pulses have been investigated extensively, as reviewed in refs 16 and 17. Extending these investigations into the soft X-

Received: June 8, 2015
Accepted: July 10, 2015
Published: July 10, 2015

DOI: 10.1021/acs.jpclett.5b01205
J. Phys. Chem. Lett. 2015, 6, 2944−2949

ray range, up to photon energies of 2 keV at LCLS, revealed novel phenomena, such as multiple core hole creation,[18−22] frustrated X-ray absorption,[18,23] and competition between inner-shell photoionization−Auger cycles and molecular dissociation.[24,25] Recently, the observations have been extended to harder X-rays (5−15 keV) at SACLA for probing femtosecond-scale atomic processes.[26,27] These studies highlighted the relevance of ultrafast deep inner-shell electron dynamics of heavy atoms in the hard X-ray range, demonstrating that they need to be taken into account for X-ray imaging in this range. Obviously, nuclear dynamics will also be relevant for hard X-ray imaging, but similar studies on molecular targets, using X-rays beyond 5 keV, common for X-ray imaging, have not yet been reported.

Here, we investigate electronic and molecular dynamics of methyl iodide (CH_3I) molecules, as a prototypical example of small organic molecules containing a heavy atom, using 5.5 keV X-ray pulses at SACLA. By comparing the observed momentum correlations of the fragment ions with a simple simulation, we demonstrate that ultrafast photoionization and Auger decay cycles produce high charge states up to +22, and that proton emission and C−I bond breaking both take place within the ultrashort X-ray pulse of 10 fs. Therefore, the present work clearly illustrates that ultrafast electron dynamics and ultrafast molecular dynamics both need to be taken into account for accurate structure retrieval in cases when ultrahigh intensity and ultrashort XFEL pulses are used and lead to a Coulomb explosion regime.

In the experiment, we have measured momenta of fragment ions using a multicoincidence spectrometer; we applied a momentum filter to extract I^{m+}−C^{n+} ion-pairs from a single CH_3I molecule based on the momentum conservation law. Namely, if five ions, I^{m+}, C^{n+}, and three protons are produced from a single CH_3I molecule, the direction of the momentum sum for the three protons is parallel to the C−I axis of the molecule. Then, one can apply the momentum conservation law for I^{m+}−C^{n+} ion pairs as follows:

$$k_{mn} \times p(I^{m+}) + p(C^{n+}) = 0 \quad (1)$$

where $p(I^{m+})$ and $p(C^{n+})$ are the momenta of I^{m+} and C^{n+}, respectively, and k_{mn} is a momentum correlation coefficient ($k_{mn} < 1$) that accounts for the "missing" momentum of the protons. Details of the momentum filtering procedure are described in the Supporting Information. The coefficients k_{mn} determined from the experimental data are plotted in Figure 1 and are compared with the predictions from a Coulomb explosion model. Its details will be given after the presentation of the experimental results, but briefly, the predictions are based on two scenarios: (a) the final charge is created instantaneously on all atoms and (b) nuclear motion is modeled on explicitly time-dependent electronic potentials that simulate the gradual buildup of charge and its transfer between atoms during the Coulomb explosion dynamics. In both cases we assumed pure Coulomb potentials for the electronic potentials and carried out the numerical integration of the equations of motion. Both are given in Figure 1.

Figure 2a depicts the charge state distribution of momentum-correlated iodine and carbon ion pairs. We have extracted, from single molecules, the I^{m+}−C^{n+} ion pairs up to $m = 15$ and $n = 4$. Taking three proton emissions into account, one can estimate the total charge of the ions released from a single molecule by the rule: $m + n + 3$. Figure 2b presents the total charge distribution, showing the maximum total charge to be equal to

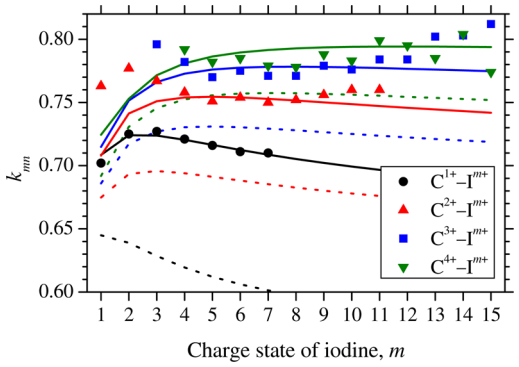

Figure 1. Momentum correlation coefficient k_{mn} for I^{m+}−C^{n+} coincidences. Closed symbols indicate the coefficients determined from experimental data. Solid lines and dotted lines of the same color indicate $|p(C^{n+})|/|p(I^{m+})|$, calculated with the charge build-up and the instant charge creation scenarios, respectively.

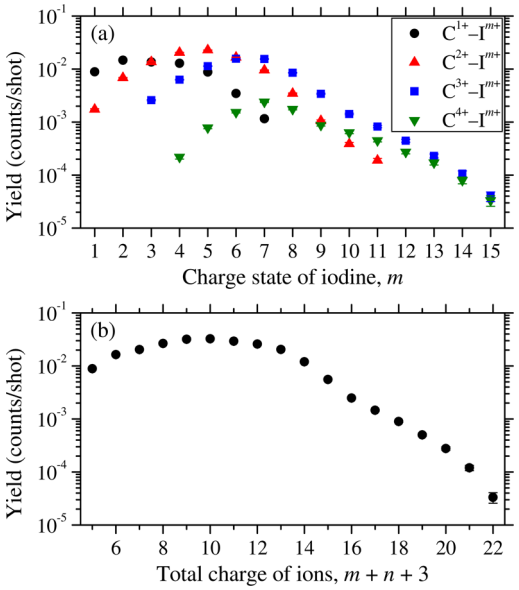

Figure 2. (a) Charge state distribution of iodine and carbon ions for I^{m+}−C^{n+} coincidences. (b) Total charge distribution of the ions released from a single molecule.

+22, as a result of multiphoton absorption and Auger cascade cycles.[26]

We obtained momentum distributions of I^{m+} and C^{n+} for each pair of charge states (m,n). As the experimental momentum values for C^{n+} ions are the most accurate due to their higher velocities, they will be used in the subsequent analysis. Figure 3 depicts the measured charge-state dependence for the momentum of carbon ions. The plotted values were obtained by three different methods: (i) as the mean of the measured 3D momentum distributions, (ii) as the position at the maximum of the 3D distribution and, independently, (iii) from the 2D momentum projection on the imaging detector via inverse Abel transformation. The three sets of values are in a good agreement, and they are all plotted providing an estimate for method-dependent systematic errors. The statistical errors are smaller than these systematic differences for all but the most highly charged ion pairs. Via I^{m+}−C^{n+}−H^+ momentum correlations, we have also extracted the angle between the direction of the proton ejection and the molecular axis

DOI: 10.1021/acs.jpclett.5b01205
J. Phys. Chem. Lett. 2015, 6, 2944−2949

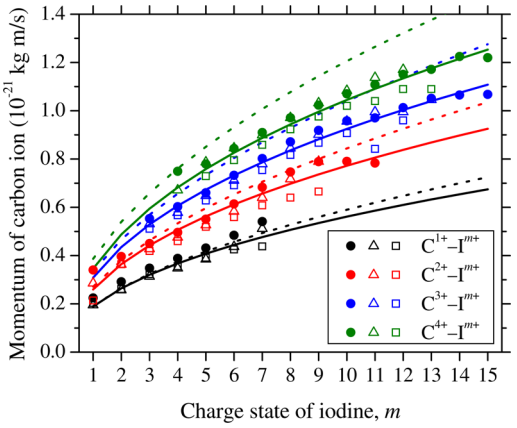

Figure 3. Momentum of carbon ions in I^{m+}–C^{n+} coincident pairs. Closed circles: means of 3D momentum distributions; open triangles: positions of the maxima of the 3D distributions; open rectangles: values from 2D distributions. Lines: predictions of the models as in Figure 1.

(determined by the I^{m+}–C^{n+} momentum correlation), as depicted in Figure 4.

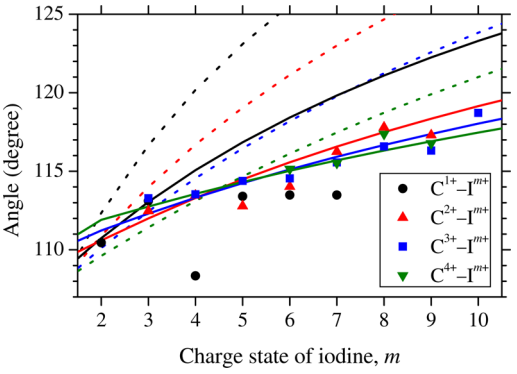

Figure 4. Angle between the direction of the proton ejection and the molecular axis determined from the I^{m+}–C^{n+} momentum correlation. Symbols: experiment; lines: predictions of the models as in Figure 1.

The dotted lines in Figures 1, 3, and 4 represent the instantaneous charge creation scenario. It fails completely in reproducing the experiment for the momentum correlation coefficients and proton emission angles, while the discrepancies are less severe for the absolute values of the momenta. This outcome requires that a realistic charge dynamics be incorporated in the model, i.e., turning to the gradual charge build-up and transfer scenario is needed. This task can be approached by solving a system of rate equations of the involved transitions, but since this is a redoubtable task for deep-core multiphoton absorption, it can be replaced by a Monte Carlo type approach.[26] However, this approach still requires a large number of time constants and probabilities, which are often poorly known. Here, we investigate a third possibility: replacing this large set of parameters with just a few generalized parameters, describing the simultaneous charge buildup and transfer, while recapturing all the experimental findings.

In the present experiment, a few photons were absorbed within the XFEL pulse duration by the deep atomic inner shells (mainly the L-shell) of iodine. In parallel and partly also subsequent to the XFEL pulse, Auger cascades are an efficient mechanism of charge multiplication, with a large number of decay channels available. While the charge creation rate by the primary photoabsorption is approximately constant within the pulse (neglecting, as explained later, the frustrated absorption effects[18,23]), the Auger processes generate charges by an exponentially decreasing rate. These numerous processes together can be fairly well represented statistically by assuming that the total charge of a molecule, Q_{total}, increases with time as

$$Q_{total}(t) = (m + n + 3) \times \left(1 - \exp\left(-\frac{t}{\tau}\right)\right) \quad (2)$$

where τ is a charge build-up time constant. Then, charge transfer within the molecule also needs to be accounted for. In our model, the total charge is divided between the iodine atom and the methyl group:

$$Q_{total}(t) = Q_I(t) + Q_{CH_3}(t) \quad (3)$$

where Q_I and Q_{CH_3} are the charges localized at the iodine atom and the methyl group, respectively. In addition we also assume that Q_{CH_3} increases up to $(n + 3)$ with a rate that is proportional to the iodine charge.

$$\frac{dQ_{CH_3}(t)}{dt} = R \times Q_I(t) \quad (4)$$

where R is a rate constant corresponding to the charge transfer. In essence, the above equations represent the initial charge creation in the strong absorber, iodine, and the subsequent charge distribution over the molecule, e.g., as a result of the charge redistribution of screening electrons from the surrounding to the iodine atom and/or the molecular Auger decay. For further charge localization within the methyl group, it was assumed that the carbon atom and the three hydrogen atoms are charged symmetrically with a fractional charge build-up until the hydrogen atoms' charges become unity. However, in cases when singly charged carbon ions are produced, the possibility that one or more neutral hydrogens are produced was taken into account by reducing the final charges to fractional values.

The best agreement between model and experiment in Figures 1, 3, and 4 was achieved using the charge build-up time τ = 9 fs and the charge transfer rate R = 0.37 fs^{-1}. The final H charge was limited to +0.77 in processes with C^+ production.

What does the generalized constant τ = 9 fs tell us about the actual charge dynamics? During the XFEL pulse duration of 10 fs, the molecule achieves about 2/3 of its final charge, indicating that the present experiment lies in the intermediate regime where both the sequential absorption and the internal decay influence the charge build-up time scale. The iodine 2s core-hole lifetime is 0.3 fs,[28] increasing toward the value of 3.3 fs for the 4d holes.[29] The iodine L-shell holes (the main result of the photoabsorption) are filled so quickly by the first steps of the Auger cascades that the frustrated absorption effect is expected to be unimportant for the charge states reached in this experiment. The final steps of the cascades are much slower and, since after the first cascades the valence shell becomes depleted, can slow down even more, carrying the final charge build-up well beyond the end of the ionizing pulse. The build-up time constant τ thus incorporates both pulse duration and Auger lifetimes. By contrast, in a long-pulse (100 fs) experiment such as that described in ref 30, the core-hole

DOI: 10.1021/acs.jpclett.5b01205
J. Phys. Chem. Lett. 2015, 6, 2944–2949

decay time has a negligible effect on the total dynamics and the value of τ.

A key feature of our model is to *simultaneously* integrate charge and nuclear dynamics. In the example of the C^{4+}–I^{10+} pair, by the end of the 10 fs pulse, the C–I bond has increased only by ≈10%, whereas the C–H distances have tripled (in the model, in each actual event large variations are expected) and thus, the hydrogen dynamics and charging is essentially complete. At this point, the C ion has acquired only about 8% of its final momentum, but the correlation coefficient k is at 50% of asymptotically reaching its final value (at 20 fs, p(C) has 66% and k 94% of its final value). The subsequent dynamics is essentially the C–I two-body dynamics with residual charging of iodine due to Auger cascades and diminishing charge transfer to the carbon ion.

As seen above, the coefficient k that represents the "missing" momentum of the hydrogens is very sensitive to the early stages of the Coulomb explosion, whereas the momenta of the heavy atoms are built-up during a much longer time period. Therefore, experimental information on both momentum correlations and their absolute values is essential for constructing useful models. However, one should be cautious when applying such statistical models to very low charge states, since the gradual charge build-up leading asymptotically to the final value clearly becomes inadequate. This limitation is perhaps most visible in Figure 4, where the charge build-up scenario does not achieve a good agreement with experiment for charge states with C^+. These are the cases where the neutral H ejection destroys the high symmetry of the triple proton ejection, and this is not fully recovered simply by the introduction of fractional charges.

The usefulness of the models with a few empirical parameters comes from their applicability to other similar systems with minimal computational effort. The present model was tested on the methylselenol molecule, allowing comparison with the results obtained by Erk et al. with very short, 5 fs XFEL pulses.[25] Starting from the set of parameters that gave the best agreement for CH_3I, we obtained a good agreement with the reported kinetic energy release (KER) values of the Se and C ions by reducing τ slightly to 8.5 fs. This is a good indication that reducing the pulse duration even further would have only minor effects on the charge dynamics, which becomes governed by the time constants of the Auger processes. In ref 25, it was concluded that the C–Se distance becomes elongated by ≈50% within the first 5 to 10 fs—a crucial conclusion from the viewpoint of molecular imaging. This conclusion is indeed also reached by our model using the instantaneous charge creation scenario, but elongating the initial C–Se distance until KERs are sufficiently reduced. In a striking contrast, when charge dynamics is switched on, our model predicts the elongation of the C–Se bond by only a few percent during 10 fs (as for the C–I bond in CH_3I). This underlines the need for an adequate treatment of the concerted charge and nuclear dynamics when considering the questions relevant to molecular imaging.

In another recent, near-infrared (NIR) pump–X-ray probe experiment, the charge transfer from iodine to the methyl group was interpreted using the classical over-the-barrier model (see ref 30 and references therein). In that model, the electron transfer is abruptly cut off at certain charge-dependent, critical C–I bond lengths. Similar findings were also made in an EUV pump–EUV probe experiment for I_2 molecules.[31] An important distinction between these pump–probe experiments and the present single-pulse one is that here the charge build-up starts immediately, whereas in refs 30 and 31 the molecule has had time to dissociate after the pump pulse, which actually initiates the dynamics.

In conclusion, we investigated the multiple ionization of the CH_3I molecule using 5.5 keV X-ray free-electron laser pulses provided by SACLA in Japan and measured momentum correlations of fragment ions using coincidence techniques. We introduced a Coulomb explosion model with a few physically meaningful empirical constants that accounts for the concerted nuclear and charge creation and transfer dynamics; the model was able to reproduce all the experimental findings with good accuracy, given its simplicity. The study demonstrates that including realistic charge dynamics is imperative when molecular Coulomb explosion experiments using short-pulse facilities are performed. It also showed that for CH_3I and CH_3SeH, this can be achieved with a simple model instead of a large set of rate equations and/or Monte Carlo methods. We hope that such models and their developments would also provide a good and efficient starting point for analyzing much larger systems, once the most useful definition of the empirical parameters and their typical values become established. Furthermore, the present results have implications not only for experiments concerned with the dissociation end products, but also for molecular imaging in which the dynamics within the pulse is relevant. For accurate estimates of nuclear motion during short ionizing pulses, it is crucial to properly treat the charge dynamics, as oversimplified estimates can be severely misleading. The present study provides by no means the final recipe, but we expect that similar empirical parametric models will play a useful role in future experiments.

■ EXPERIMENTAL METHOD

The experiment has been carried out at the experimental hutch 3 (EH3) of the beamline 3 (BL3) of SACLA.[17,32] The XFEL beam is focused to a focal size of ∼1 μm (fwhm) in diameter.[33] The gas phase sample was introduced to the focal point of the XFEL pulses as a pulsed supersonic gas jet seeded by helium gas. The gas beam at the reaction point was estimated to be ∼3 mm (fwhm) in diameter, i.e., shorter than the Rayleigh length of ∼8 mm. Thus, the ions' source volume was a cylindrical shape of ∼1 μm in diameter and ∼3 mm along the XFEL beam.

The photon energy was set at 5.5 keV, and the photon bandwidth was ∼40 eV (fwhm). The repetition rate of the XFEL pulses was 10 Hz. The pulse length was estimated to be ∼10 fs (fwhm).[34] FEL pulse energies were measured by the beam-position monitor[35] located upstream of the beamline and calibrated by a calorimeter.[36] The measured value was 235 μJ per pulse in average. Note that the pulse energy is not measured at the interaction point but upstream, and that losses occur due to beam transport and diagnostics. The relative X-ray pulse energy at the interaction point was also measured shot-by-shot by a p-intrinsic-n (PIN) photodiode. The shot-by-shot pulse energy fluctuation was ±7% (14% fwhm). The peak fluence at the interaction point was 26 $\mu J/\mu m^2$ in average. The absolute value of the peak fluence was determined just after the experiment via a well-established calibration procedure using argon.[26,37]

Ions produced in the source volume described above were extracted toward an ion momentum spectrometer equipped with microchannel plates (MCP) and a delay-line anode (Roentdek HEX80).[38] We used velocity-map-imaging (VMI)[39] electric field conditions. Signals from the delay-line anode and MCP were recorded by a digitizer and analyzed by a software

DOI: 10.1021/acs.jpclett.5b01205
J. Phys. Chem. Lett. 2015, 6, 2944–2949

discriminator.[40] The arrival time and the arrival position of each ion were determined and allowed us to extract the 3D momentum of each ion (see ref 41 and refereces therein). With the voltage settings of the spectrometer, we could extract all I^{m+} and C^{n+} ions ejected in all directions, whereas protons with kinetic energies above ~80 eV could not be fully collected. Only few polyatomic fragments were observed. The contribution of those fragments to the topic discussed here was negligible. An example of a time-of-flight mass spectrum is given in the Supporting Information for illustration.

■ ASSOCIATED CONTENT

Supporting Information

Details of the momentum filtering procedure are described. The Supporting Information is available free of charge on the ACS Publications website at DOI: 10.1021/acs.jpclett.5b01205.

■ AUTHOR INFORMATION

Corresponding Author

*Phone:+81-(0)22-217-5381; Fax:+81-(0)22-217-5380; E-mail: ueda@tagen.tohoku.ac.jp.

Author Contributions

K. Motomura and E. Kukk contributed equally to this work.

Notes

The authors declare no competing financial interest.

■ ACKNOWLEDGMENTS

The experiments were performed at SACLA with the approval of JASRI and the program review committee (No. 2012B8045). This study was supported by the X-ray Free Electron Laser Utilization Research Project and the X-ray Free Electron Laser Priority Strategy Program of the Ministry of Education, Culture, Sports, Science and Technology of Japan (MEXT), by the Japan Society for the Promotion of Science (JSPS) KAKENHI Grant No. 21244062, No. 23241033, by MEXT KAKENHI Grant No. 22740264, by the Proposal Program of SACLA Experimental Instruments of RIKEN, by the Academy of Finland, and by the Cooperative Research Program of the Network Joint Research Center for Materials and Devices of MEXT. A.R. was supported by the Chemical Sciences, Geosciences, and Biosciences Division of the Office of Basic Energy Sciences, Office of Science, U.S. Department of Energy. C.M. and C.N. acknowledge support from the CNRS program PEPS "SASELELX"; E.K. and C.M. acknowledge support from the European Cooperation in Science and Technology (COST) action CM1204 - XUV/x-ray light and fast ions for ultrafast chemistry (XLIC). S.M. acknowledges financial support from JSPS. Y.H.J. is grateful for support from the National Basic Research Program of China (Grant 2013CB922200), the NSFC (Grant No. 11274232 and 11420101003), and the Shanghai Pujiang Program (Grant 13PJ1407500). D.K. and M.A. are grateful for the support from the Global Research Laboratory Program (Grant No. 2009-00439) and Max Planck POSTECH/KOREA Research Initiative Program (Grant No. 2011-0031558) through the National Research Foundation of Korea (NRF) funded by the Ministry of Science, ICT & Future Planning.

■ REFERENCES

(1) Emma, P.; Akre, R.; Arthur, J.; Bionta, R.; Bostedt, C.; Bozek, J.; Brachmann, A.; Bucksbaum, P.; Coffee, R.; Decker, F.-J.; et al. First Lasing and Operation of an Ångstrom-Wavelength Free-Electron Laser. *Nat. Photonics* **2010**, *4*, 641−647.

(2) Ishikawa, T.; Aoyagi, H.; Asaka, T.; Asano, Y.; Azumi, N.; Bizen, T.; Ego, H.; Fukami, K.; Fukui, T.; Furukawa, Y.; et al. A Compact X-ray Free-Electron Laser Emitting in the Sub-Ångström Region. *Nat. Photonics* **2012**, *6*, 540−544.

(3) Seibert, M. M.; Ekeberg, T.; Maia, F. R. N. C.; Svenda, M.; Andreasson, J.; Jönsson, O.; Odić, D.; Iwan, B.; Rocker, A.; Westphal, D.; et al. Single Mimivirus Particles Intercepted and Imaged with an X-ray Laser. *Nature* **2011**, *470*, 78−81.

(4) Loh, N. D.; Hampton, C. Y.; Martin, A. V.; Starodub, D.; Sierra, R. G.; Barty, A.; Aquila, A.; Schulz, J.; Lomb, L.; Steinbrener, J.; et al. Fractal Morphology, Imaging and Mass Spectrometry of Single Aerosol Particles in Flight. *Nature* **2012**, *486*, 513−517.

(5) Gorkhover, T.; Adolph, M.; Rupp, D.; Schorb, S.; Epp, S. W.; Erk, B.; Foucar, L.; Hartmann, R.; Kimmel, N.; Kühnel, K.-U.; et al. Nanoplasma Dynamics of Single Large Xenon Clusters Irradiated with Superintense X-ray Pulses from the Linac Coherent Light Source Free-Electron Laser. *Phys. Rev. Lett.* **2012**, *108*, 245005.

(6) Takahashi, Y.; Suzuki, A.; Zettsu, N.; Oroguchi, T.; Takayama, Y.; Sekiguchi, Y.; Kobayashi, A.; Yamamoto, M.; Nakasako, M. Coherent Diffraction Imaging Analysis of Shape-Controlled Nanoparticles with Focused Hard X-ray Free-Electron Laser Pulses. *Nano Lett.* **2013**, *13*, 6028−6032.

(7) Kimura, T.; Joti, Y.; Shibuya, A.; Song, C.; Kim, S.; Tono, K.; Yabashi, M.; Tamakoshi, M.; Moriya, T.; Oshima, T.; et al. Imaging Live Cell in Micro-Liquid Enclosure by X-ray Laser Diffraction. *Nat. Commun.* **2014**, *5*, 3052.

(8) Chapman, H. N.; Fromme, P.; Barty, A.; White, T. A.; Kirian, R. A.; Aquila, A.; Hunter, M. S.; Schulz, J.; DePonte, D. P.; Weierstall, U.; et al. Femtosecond X-ray Protein Nanocrystallography. *Nature* **2011**, *470*, 73−77.

(9) Boutet, S.; Lomb, L.; Williams, G. J.; Barends, T. R. M.; Aquila, A.; Doak, R. B.; Weierstall, U.; DePonte, D. P.; Steinbrener, J.; Shoeman, R. L.; et al. High-Resolution Protein Structure Determination by Serial Femtosecond Crystallography. *Science* **2012**, *337*, 362−364.

(10) Redecke, L.; Nass, K.; DePonte, D. P.; White, T. A.; Rehders, D.; Barty, A.; Stellato, F.; Liang, M.; Barends, T. R. M.; Boutet, S.; et al. Natively Inhibited Typanosoma brucei Cathepsin B Structure Determined by Using an X-ray Laser. *Science* **2013**, *339*, 227−230.

(11) Barends, T. R. M.; Foucar, L.; Shoeman, R. L.; Bari, S.; Epp, S. W.; Hartmann, R.; Hauser, G.; Huth, M.; Kieser, C.; Lomb, L.; et al. Anomalous Signal from S Atoms in Protein Crystallographic Data from an X-ray Free-Electron Laser. *Acta Crystallogr., Sect. D: Biol. Crystallogr.* **2013**, *69*, 838−842.

(12) Barends, T. R. M.; Foucar, L.; Botha, S.; Doak, R. B.; Shoeman, R. L.; Nass, K.; Koglin, J. E.; Williams, G. J.; Boutet, S.; Messerschmidt, M.; et al. De Novo Protein Crystal Structure Determination from X-ray Free-Electron Laser Data. *Nature* **2014**, *505*, 244−247.

(13) Quiney, H. M.; Nugent, K. A. Biomolecular Imaging and Electronic Damage Using X-ray Free-Electron Lasers. *Nat. Phys.* **2011**, *7*, 142−146.

(14) Barty, A.; Caleman, C.; Aquila, A.; Timneanu, N.; Lomb, L.; White, T. A.; Andreasson, J.; Arnlund, D.; Bajt, S.; Barends, T. R. M.; et al. Self-Terminating Diffraction Gates Femtosecond X-ray Nanocrystallography Measurements. *Nat. Photonics* **2012**, *6*, 35−40.

(15) Lomb, L.; Barends, T. R. M.; Kassemeyer, S.; Aquila, A.; Epp, S. W.; Erk, B.; Foucar, L.; Hartmann, R.; Rudek, B.; Rolles, D.; et al. Radiation Damage in Protein Serial Femtosecond Crystallography Using an X-ray Free-Electron Laser. *Phys. Rev. B: Condens. Matter Mater. Phys.* **2011**, *84*, 214111.

(16) Feldhaus, J.; Krikunova, M.; Meyer, M.; Möller, Th.; Moshammer, R.; Rudenko, A.; Tschentscher, Th.; Ullrich, J. AMO Science at the FLASH and European XFEL Free-Electron Laser Facilities. *J. Phys. B: At., Mol. Opt. Phys.* **2013**, *46*, 164002.

(17) Yabashi, M.; Tanaka, H.; Tanaka, T.; Tomizawa, H.; Togashi, T.; Nagasono, M.; Ishikawa, T.; Harries, J. R.; Hikosaka, Y.; Hishikawa,

DOI: 10.1021/acs.jpclett.5b01205
J. Phys. Chem. Lett. 2015, 6, 2944−2949

A.; et al. Compact XFEL and AMO Sciences: SACLA and SCSS. *J. Phys. B: At., Mol. Opt. Phys.* **2013**, *46*, 164001.
(18) Young, L.; Kanter, E. P.; Krässig, B.; Li, Y.; March, A. M.; Pratt, S. T.; Santra, R.; Southworth, S. H.; Rohringer, N.; DiMauro, L. F.; et al. Femtosecond Electronic Response of Atoms to Ultra-Intense X-rays. *Nature* **2010**, *466*, 56−61.
(19) Rudek, B.; Son, S.-K.; Foucar, L.; Epp, S. W.; Erk, B.; Hartmann, R.; Adolph, M.; Andritschke, R.; Aquila, A.; Berrah, N.; et al. Ultra-Efficient Ionization of Heavy Atoms by Intense X-ray Free-Electron Laser Pulses. *Nat. Photonics* **2012**, *6*, 858−865.
(20) Frasinski, L. J.; Zhaunerchyk, V.; Mucke, M.; Squibb, R. J.; Siano, M.; Eland, J. H. D.; Linusson, P.; Meulen, P. v. d.; Salén, P.; Thomas, R. D.; et al. Dynamics of Hollow Atom Formation in Intense X-ray Pulses Probed by Partial Covariance Mapping. *Phys. Rev. Lett.* **2013**, *111*, 073002.
(21) Berrah, N.; Fang, L.; Murphy, B.; Osipov, T.; Ueda, K.; Kukk, E.; Feifel, R.; Meulen, P. v. d.; Salen, P.; Schmidt, H. T.; et al. Double-Core-Hole Spectroscopy for Chemical Analysis with an Intense X-ray Femtosecond Laser. *Proc. Natl. Acad. Sci. U. S. A.* **2011**, *108*, 16912−16915.
(22) Salén, P.; van der Meulen, P.; Schmidt, H. T.; Thomas, R. D.; Larsson, M.; Feifel, R.; Piancastelli, M. N.; Fang, L.; Murphy, B.; Osipov, T.; et al. Experimental Verification of the Chemical Sensitivity of Two-Site Double Core-Hole States Formed by an X-ray Free-Electron Laser. *Phys. Rev. Lett.* **2012**, *108*, 153003.
(23) Hoener, M.; Fang, L.; Kornilov, O.; Gessner, O.; Pratt, S. T.; Gühr, M.; Kanter, E. P.; Blaga, C.; Bostedt, C.; Bozek, J. D.; et al. Ultraintense X-ray Induced Ionization, Dissociation, and Frustrated Absorption in Molecular Nitrogen. *Phys. Rev. Lett.* **2010**, *104*, 253002.
(24) Fang, L.; Osipov, T.; Murphy, B.; Tarantelli, F.; Kukk, E.; Cryan, J. P.; Glownia, M.; Bucksbaum, P. H.; Coffee, R. N.; Chen, M.; et al. Multiphoton Ionization as a Clock to Reveal Molecular Dynamics with Intense Short X-ray Free Electron Laser Pulses. *Phys. Rev. Lett.* **2012**, *109*, 263001.
(25) Erk, B.; Rolles, D.; Foucar, L.; Rudek, B.; Epp, S. W.; Cryle, M.; Bostedt, C.; Schorb, S.; Bozek, J.; Rouzee, A.; et al. Ultrafast Charge Rearrangement and Nuclear Dynamics upon Inner-Shell Multiple Ionization of Small Polyatomic Molecules. *Phys. Rev. Lett.* **2013**, *110*, 053003.
(26) Fukuzawa, H.; Son, S.-K.; Motomura, K.; Mondal, S.; Nagaya, K.; Wada, S.; Liu, X.-J.; Feifel, R.; Tachibana, T.; Ito, Y.; et al. Deep Inner-Shell Multiphoton Ionization by Intense X-ray Free-Electron Laser Pulses. *Phys. Rev. Lett.* **2013**, *110*, 173005.
(27) Tamasaku, K.; Nagasono, M.; Iwayama, H.; Shigemasa, E.; Inubushi, Y.; Tanaka, T.; Tono, K.; Togashi, T.; Sato, T.; Katayama, T.; et al. Double Core-Hole Creation by Sequential Attosecond Photoionization. *Phys. Rev. Lett.* **2013**, *111*, 043001.
(28) Erk, B. Fragmentation Dynamics of Small Molecules upon Multiple Ionization by X-ray Free-Electron Laser Pulses. Ph.D. Thesis, The Ruperto-Carola-University of Heidelberg, January 2013.
(29) Cutler, J. N.; Bancroft, G. M.; Tan, K. H. Ligand-Field Splittings and Core-Level Linewidths in I 4d Photoelectron Spectra of Iodine Molecules. *J. Chem. Phys.* **1992**, *97*, 7932−7943.
(30) Erk, B.; Boll, R.; Trippel, S.; Anielski, D.; Foucar, L.; Rudek, B.; Epp, S. W.; Coffee, R.; Carron, S.; Schorb, S.; et al. Imaging Charge Transfer in Iodomethane upon X-ray Photoabsorption. *Science* **2014**, *345*, 288−291.
(31) Schnorr, K.; Senftleben, A.; Kurka, M.; Rudenko, A.; Schmid, G.; Pfeifer, T.; Meyer, K.; Kübel, M.; Kling, M. F.; Jiang, Y. H.; et al. Electron Rearrangement Dynamics in Dissociating I_2^{n+} Molecules Accessed by Extreme Ultraviolet Pump-Probe Experiments. *Phys. Rev. Lett.* **2014**, *113*, 073001.
(32) Tono, K.; Togashi, T.; Inubushi, Y.; Sato, T.; Katayama, T.; Ogawa, K.; Ohashi, H.; Kimura, H.; Takahashi, S.; Takeshita, K.; et al. Beamline, Experimental Stations and Photon Beam Diagnostics for the Hard X-ray Free Electron Laser of SACLA. *New J. Phys.* **2013**, *15*, 083035.
(33) Yumoto, H.; Mimura, H.; Koyama, T.; Matsuyama, S.; Tono, K.; Togashi, T.; Inubushi, Y.; Sato, T.; Tanaka, T.; Kimura, T.; et al. Focusing of X-ray Free-Electron Laser Pulses with Reflective Optics. *Nat. Photonics* **2013**, *7*, 43−47.
(34) Inubushi, Y.; Tono, K.; Togashi, T.; Sato, T.; Hatsui, T.; Kameshima, T.; Togawa, K.; Hara, T.; Tanaka, T.; Tanaka, H.; et al. Determination of the Pulse Duration of an X-ray Free Electron Laser Using Highly Resolved Single-Shot Spectra. *Phys. Rev. Lett.* **2012**, *109*, 144801.
(35) Tono, K.; Kudo, T.; Yabashi, M.; Tachibana, T.; Feng, Y.; Fritz, D.; Hastings, J.; Ishikawa, T. Single-Shot Beam-Position Monitor for X-ray Free Electron Laser. *Rev. Sci. Instrum.* **2011**, *82*, 023108.
(36) Kato, M.; Tanaka, T.; Kurosawa, T.; Saito, N.; Richter, M.; Sorokin, A. A.; Tiedtke, K.; Kudo, T.; Tono, K.; Yabashi, M.; et al. Pulse Energy Measurement at the Hard X-ray Laser in Japan. *Appl. Phys. Lett.* **2012**, *101*, 023503.
(37) Motomura, K.; Fukuzawa, H.; Son, S.-K.; Mondal, S.; Tachibana, T.; Ito, Y.; Kimura, M.; Nagaya, K.; Sakai, T.; Matsunami, K.; et al. Sequential Multiphoton Multiple Ionization of Atomic Argon and Xenon Irradiated by X-ray Free-Electron Laser Pulses from SACLA. *J. Phys. B: At., Mol. Opt. Phys.* **2013**, *46*, 164024.
(38) Jagutzki, O.; Cerezo, A.; Czasch, A.; Dörner, R.; Hattaß, M.; Huang, M.; Mergel, V.; Spillmann, U.; Ullmann-Pfleger, K.; Weber, T.; et al. Multiple Hit Readout of a Microchannel Plate Detector With a Three-Layer Delay-Line Anode. *IEEE Trans. Nucl. Sci.* **2002**, *49*, 2477−2483.
(39) Eppink, A. T. J. B.; Parker, D. H. Velocity Map Imaging of Ions and Electrons Using Electrostatic Lenses: Application in Photoelectron and Photofragment Ion Imaging of Molecular Oxygen. *Rev. Sci. Instrum.* **1997**, *68*, 3477−3484.
(40) Motomura, K.; Foucar, L.; Czasch, A.; Saito, N.; Jagutzki, O.; Schmidt-Böcking, H.; Dörner, R.; Liu, X.-J.; Fukuzawa, H.; Prümper, G.; et al. Multi-Coincidence Ion Detection System for EUV-FEL Fragmentation Experiments at SPring-8. *Nucl. Instrum. Methods Phys. Res., Sect. A* **2009**, *606*, 770−773.
(41) Ueda, K.; Eland, J. H. D. Molecular Photodissociation Studied by VUV and Soft X-ray Radiation. *J. Phys. B: At., Mol. Opt. Phys.* **2005**, *38*, S839−S859.

DOI: 10.1021/acs.jpclett.5b01205
J. Phys. Chem. Lett. 2015, 6, 2944−2949